Eur. Phys. J. A **25**, s01, 589–594 (2005)
DOI: 10.1140/epjad/i2005-06-134-9

EPJ A direct
electronic only

New elements from Dubna

Yu.Ts. Oganessian[1], V.K. Utyonkov[1,a], Yu.V. Lobanov[1], F.Sh. Abdullin[1], A.N. Polyakov[1], I.V. Shirokovsky[1], Yu.S. Tsyganov[1], G.G. Gulbekian[1], S.L. Bogomolov[1], B.N. Gikal[1], A.N. Mezentsev[1], S. Iliev[1], V.G. Subbotin[1], A.M. Sukhov[1], A.A. Voinov[1], G.V. Buklanov[1], K. Subotic[1], V.I. Zagrebaev[1], M.G. Itkis[1], J.B. Patin[2], K.J. Moody[2], J.F. Wild[2], M.A. Stoyer[2], N.J. Stoyer[2], D.A. Shaughnessy[2], J.M. Kenneally[2], P.A. Wilk[2], and R.W. Lougheed[2]

[1] Joint Institute for Nuclear Research, 141980 Dubna, Russian Federation
[2] University of California, Lawrence Livermore National Laboratory, Livermore, CA 94551, USA

Received: 19 October 2004 /
Published online: 29 June 2005 –

Abstract. We have studied the dependence of the production cross-sections of the isotopes ^{282,283}112 and $^{286-288}$114 on the excitation energy of the compound nuclei ^{286}112 and ^{290}114. The maximum cross-sections of the xn-evaporation channels for the reaction ^{238}U(^{48}Ca, xn)$^{286-x}$112 were measured to be: $\sigma_{3n} = 2.5^{+1.8}_{-1.1}$ pb and $\sigma_{4n} = 0.6^{+1.6}_{-0.5}$ pb; for the reaction ^{242}Pu(^{48}Ca, xn)$^{290-x}$114: $\sigma_{2n} \sim 0.5$ pb, $\sigma_{3n} = 3.6^{+3.4}_{-1.7}$ pb and $\sigma_{4n} = 4.5^{+3.6}_{-1.9}$ pb. In the reaction ^{233}U(^{48}Ca, 2–4n)$^{277-279}$112 we measured an upper cross-section limit of $\sigma_{xn} \leq 0.6$ pb. An increase of σ_{ER} in the reactions of actinide targets with ^{48}Ca can be due to the expected increase of the survivability of the excited compound nucleus upon closer approach to the closed neutron shell $N = 184$. The observed nuclear decay properties of the nuclides with $Z = 104$–118 are compared with theoretical nuclear mass calculations and the systematic trends of α-decay properties. As a whole, they give a consistent pattern of decay of the 18 even-Z neutron-rich nuclides with $Z = 104$–118 and $N = 163$–177.

PACS. 25.70.Gh Compound nucleus – 23.60.+e α decay – 25.85.Ca Spontaneous fission – 27.90.+b $220 \leq A$

1 Introduction

According to the nuclear models, the limits of the existence of the heavy nuclei, as well as their decay properties, are completely determined by nuclear shell effects. For the heaviest elements in the vicinity of the hypothetical closed spherical shells $Z = 114$ and $N = 184$, the increase of nuclear binding energy results in a considerable increase of stability with respect to various decay modes. We may also speculate that the high fission barriers of the superheavy nuclei in their ground states may persist at low excitation energies, resulting in an increase in their production cross-sections, or to be more precise their survival probability in the process of de-excitation of the compound nucleus. Both the production cross-sections and the stability of superheavy nuclides are expected to increase on closer approach to the closed neutron shell $N = 184$. Therefore, our first experiments aimed at the synthesis of the heaviest nuclei involved the complete fusion reactions ^{244}Pu, ^{248}Cm + ^{48}Ca that lead to the compound nuclei with the maximum accessible neutron numbers [1]. Following the successful completion of the experiments in which fission in ^{48}Ca-induced reactions was studied [2] we decided to investigate the survival probabilities of the compound nuclei by measuring excitation functions for producing evaporation residues (ER). The first such measurements were performed using the reaction ^{244}Pu(^{48}Ca, 3–5n)$^{287-289}$114 [3]. In the present work, we further develop these investigations with different targets: ^{233}U, ^{238}U, ^{242}Pu and ^{248}Cm, producing compound nuclei with $Z = 112$, 114 and 116.

2 Experimental technique

The ^{48}Ca-ion beam was accelerated by the U400 cyclotron at the Flerov Laboratory of Nuclear Reactions. The typical beam intensity at the target was 1.2 pμA. The 32-cm^2 rotating targets consisted of the enriched isotopes ^{233}U (99.97%), ^{238}U (99.3%), ^{242}Pu (99.98%), and ^{248}Cm (97.4%) with thicknesses of about 0.44, 0.35, 0.40, and 0.35 mg/cm^2, respectively.

The evaporation residues recoiling from the target were separated in flight by the Dubna Gas-filled Recoil Separator [4]. The transmission efficiency of the separator for $Z = 112$ and 114 nuclei is estimated to be approximately 40% [4]. ERs passed through a time-of-flight system (TOF) and were implanted in a 4×12 cm^2 semiconductor detector array with 12 vertical position-sensitive

[a] Conference presenter; e-mail: utyonkov@sungns.jinr.ru

Table 1. Reaction-specific lab-frame beam energies in the middle of the target layers, corresponding excitation energies [5] and total beam doses for the given reactions.

Reaction	E_{beam}(MeV)	E^*(MeV)	Beam dose
^{242}Pu + ^{48}Ca	235	30.4–34.7	5.0×10^{18}
	238	33.1–37.4	4.9×10^{18}
	244	38.0–42.4	4.7×10^{18}
	250	43.0–47.2	3.2×10^{18}
^{238}U + ^{48}Ca	230	29.3–33.5	5.8×10^{18}
	234	32.9–37.2	7.1×10^{18}
	240	37.7–41.9	5.2×10^{18}
^{233}U + ^{48}Ca	240	32.7–37.1	7.7×10^{18}
^{248}Cm + ^{48}Ca	247	36.8–41.1	7.0×10^{18}

strips. This detector was surrounded by eight $4\times4\,\mathrm{cm}^2$ side detectors without position sensitivity, forming a box open to the beam side. The detection efficiency for full-energy α particles emitted from implanted nuclei was 87%. The energy resolution for α particles absorbed in the focal-plane detector was 55–95 keV. The α particles that escaped the focal-plane detector at different angles and which were registered in a side detector had an energy resolution of the summed signals of 140–220 keV. The FWHM position resolutions were 0.9–1.4 mm for ER-α signals and 0.5–0.9 mm for ER-SF signals. Fission fragments from the decay of ^{252}No implants produced in the ^{206}Pb + ^{48}Ca reaction were used for their energy calibration. The measured fragment energies were not corrected for the pulse-height defect of the detectors, or for energy loss in the detectors' entrance windows, dead layers, and the pentane gas filling of the detection system. The mean sum energy loss of fission fragments was about 20 MeV.

In the experiments we employed a special low-background detection scheme for the investigated nuclides [1,3]. The beam was switched off after a recoil signal was detected with parameters of implantation energy and TOF expected for ERs, followed by an α-like signal with an energy expected for an α-particle of the mother nucleus, in the same strip, within a 1.4–1.9 mm wide position window and some preset time interval. The duration of the pause in beam was determined from the observed pattern of out-of-beam α decays and varied from 1 to 12 minutes. Thus, all the expected sequential decays of the daughter nuclides were expected to be observed in the absence of beam-associated background.

3 Experimental results

The experimental conditions are summarized in table 1. Excitation energies of the compound nuclei at given ion energies are calculated taking into account the thickness of the targets and the energy spread of the incident cyclotron beam.

In the course of the experiments with the ^{242}Pu target, performed at four bombarding energies, 25 decay chains

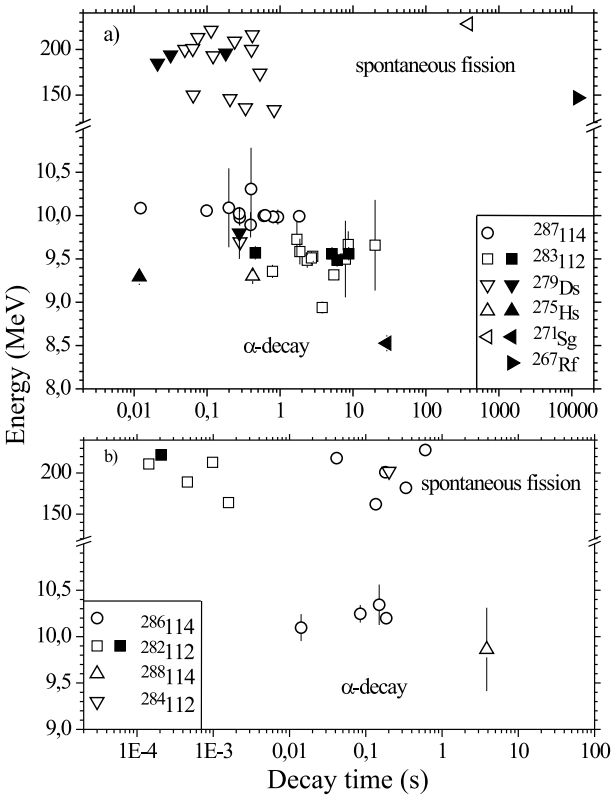

Fig. 1. a) α or SF energies and decay times of nuclei produced in the reactions ^{242}Pu(^{48}Ca, $3n$)^{287}114 (open symbols) and ^{238}U(^{48}Ca, $3n$)^{283}112 (solid symbols). b) The same for even-even isotopes ^{286}114 and ^{288}114.

were detected that we assign to the decay of $Z = 114$ nuclides. The detected energies of events and time intervals between members of decay chains are shown in fig. 1. The decay chains can be sorted into three groups: decay chains of the ER-α-α-SF type lasting for 2–20 s (one special case is an ER-α-α-α-α-SF chain lasting for 6.5 min, see fig. 2) observed at beam energies E_L = 235–244 MeV; shorter decays of the ER-α-SF or ER-SF type spanning a typical time of 0.01–0.6 s, observed at higher beam energies E_L = 244–250 MeV; and, finally, a single ER-α-SF event, $t \approx 4$ s, detected at the lowest beam energy E_L = 235 MeV. In the ^{242}Pu+^{48}Ca reaction, we detected a total of 33 α-decays in the correlated decay chains. Four α-particles are missing, which is entirely consistent with the α-detection efficiency of the detector array that is approximately 87%. In fig. 1, such events and their daughters are not shown.

In the ^{238}U + ^{48}Ca experiments, we detected 8 decay sequences that we have assigned to the decay of $Z = 112$ nuclides. These can be separated into two types: ER-α-SF chains spanning about 0.5–6 s that were observed at beam energies E_L = 230–234 MeV; and shorter ER-SF sequences with $t_{SF} < 1$ ms observed at E_L = 240 MeV. Two longer ER-α-α-α-α-SF decay chains observed in the reactions ^{242}Pu + ^{48}Ca and ^{238}U + ^{48}Ca are shown separately in fig. 2.

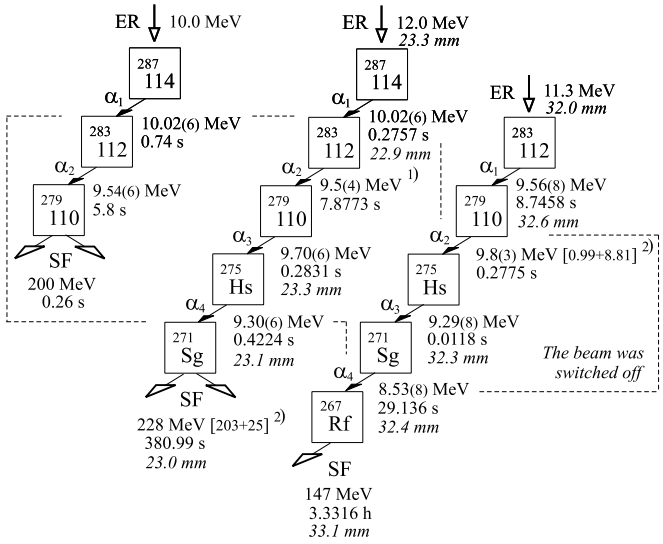

Fig. 2. Time sequences in the average decay chain of ^{287}114 (left) and in selected decay chains observed in the ^{242}Pu+^{48}Ca (middle) and ^{238}U+^{48}Ca (right) reactions. Measured energies, time intervals and positions of the observed decay events are shown. Energy uncertainties are shown in parentheses. 1) The energy of this event was detected by side detectors only. 2) The energies of events detected by both the focal-plane and side detectors, respectively, are shown in brackets.

The production cross-sections of the nuclides detected in our experiments as a function of the excitation energies of the compound nuclei ^{290}114 and ^{286}112, are shown in fig. 3. In addition, excitation functions of the reactions ^{244}Pu(^{48}Ca, 3–5n)$^{287-289}$114 that we measured earlier [3] and the available data for the reaction ^{248}Cm(^{48}Ca, 3–4n)^{292,293}116 are also shown, together with the Bass reaction barrier [6] and the calculated excitation functions [7]. Comparing the decay properties of the observed nuclei and the excitation functions for their production, we can deduce a consistent picture for the masses of the observed nuclides.

The decays of the daughter nuclei in the ER-α-α-SF chains observed in the reaction ^{242}Pu + ^{48}Ca coincides in all the measured parameters (E_α, T_α, T_{SF}, and E_{SF}) with the decay chain ER-α-SF observed in the ^{238}U + ^{48}Ca reaction. The maximum yields of the nuclides that undergo this type of decay correspond to the calculated 3n-evaporation channel in the fusion reactions ^{242}Pu, ^{238}U+^{48}Ca. Therefore, the ER-α-α-SF decay chain from the reaction ^{242}Pu + ^{48}Ca should be assigned to the decay of ^{287}114. This conclusion is supported by the data from the reactions ^{245}Cm, ^{244}Pu + ^{48}Ca in which similar decay chains were observed in 2n- and 5n evaporation channels [3], respectively. Accordingly, the ER-α-SF chains observed in the reaction ^{238}U+^{48}Ca are due to the α decay of ^{283}112 that is terminated by the spontaneous fission of the isotope ^{279}Ds ($T_{SF} = 0.18$ s).

The excitation functions and the decay properties of the shorter chain members (ER-α-SF) detected in the ^{242}Pu + ^{48}Ca reaction, and ER-SF correlations in ^{238}U + ^{48}Ca reaction, determine that these originate from

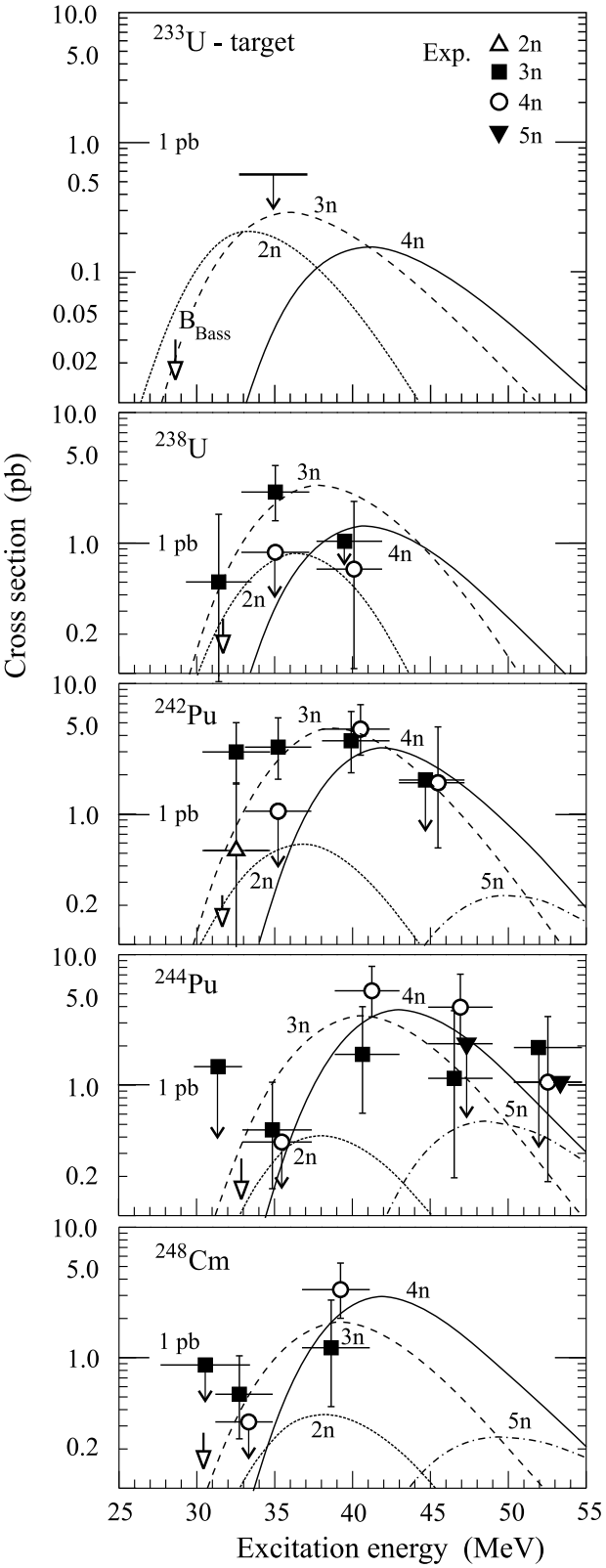

Fig. 3. Excitation functions for the 2–5n evaporation channels from the complete-fusion reactions ^{233,238}U, ^{242,244}Pu, ^{248}Cm + ^{48}Ca. The Bass barrier [6] is shown by an open arrow in each panel; in the topmost panel it is labeled with $B_{\rm Bass}$. Lines show the results of calculations [7]. Error bars correspond to statistical uncertainties.

the neighboring even-even isotopes ^{286}114 and ^{282}112, respectively. Note that in the decay of ^{286}114, as observed in all of the experiments, five α decays were observed out of thirteen atoms ($b_\alpha \approx 0.4$) [3,8]. Finally, a single ER-α-SF event observed in the reaction ^{242}Pu + ^{48}Ca at a beam energy $E_L = 235$ MeV agrees well in decay properties with the well-studied nuclide ^{288}114 (12 events detected) that we previously synthesized in the reaction ^{244}Pu + ^{48}Ca [3]. This event should then be assigned to the decay of ^{288}114 produced via $2n$ evaporation with a cross-section of about 0.5 pb.

We have also studied the reaction ^{233}U + ^{48}Ca; despite an accumulated beam dose of about 8×10^{18} ions, we did not observe any decay chains that could be attributed to the decay of isotopes of element 112. We calculate an upper cross-section limit of $\sigma_{2-4n} \leq 0.6$ pb for the reaction ^{233}U(^{48}Ca, 2–4n)$^{277-279}$112.

4 Discussion

In the ER-α-α-SF chains arising in the decay of the isotope ^{287}114, the energy of the first α-particle is $E_{\alpha 1} = 10.02 \pm 0.06$ MeV. In all 12 events in which the decay of the mother nuclide has been observed, the measured values of $E_{\alpha 1}$ agree with the given value within detector resolution, as well as with the value measured for this isotope in [3]. The energy of the second α-particle in 11 cases of 14 is $E_{\alpha 2} = 9.54 \pm 0.06$ MeV. This value, as we noted above, agrees well with the four measured α-energies of ^{283}112 (see fig. 1), produced as a fusion-evaporation product in the reaction ^{238}U(^{48}Ca, 3n)^{283}112, and with energies registered for this isotope in previous experiments [3].

However, three of the measured energies of the second alpha, $E_{\alpha 2} = 8.94(7)$, 9.36(8) and 9.32(6) MeV, are different enough from the average value of $E_{\alpha 2}$ that they are beyond the experimental uncertainties of measuring α-energies. This means that the observed α-decays of ^{283}112 correspond to transitions to various excited states in the daughter nucleus ^{279}110. Given the accuracy with which we measure the α-particle energies and the relatively low statistics, we can evaluate the probability of such transitions as being about 20%. In principle, this kind of decay pattern for an odd nucleus is possible since ^{279}110 ($N = 169$) is located in an intermediate region 7 neutrons above the deformed shell closure at $N = 162$ and 15 neutrons below the spherical shell at $N = 184$. As a whole, the decay properties of the isotope ^{283}112 produced in the reactions ^{238}U + ^{48}Ca and ^{242}Pu + ^{48}Ca do not depend on whether it is observed as a primary nucleus or as an α-decay product of a preceding mother nucleus.

At the same time, in one of the 15 decays of ^{287}114 produced in the reaction ^{242}Pu + ^{48}Ca and in one of the 7 decays of ^{283}112 produced in the reaction ^{238}U + ^{48}Ca, we observed lengthy sequential α decays that were terminated by SF with long lifetimes: $t_{SF} \approx 6.3$ min and 3.3 h, respectively, see fig. 2. These rare decays result from α/SF competition in the decay of ^{279}110 ($b_\alpha \approx 10\%$, including three decays observed in [3]) and end in the SF of the relatively neutron-rich isotopes ^{271}Sg ($N = 165$) and ^{267}Rf ($N = 163$). Comparing the two decay chains, one can see that ^{271}Sg undergoes both α decay ($E_\alpha = 8.53$ MeV) and SF.

Table 2. Decay properties of nuclei produced in this work and [1,3,8].

Isotope	$b_{\alpha/f}$(%)	$T_{1/2}^{exp.}$	$T_\alpha^{calc.}$	E_α(MeV)
^{294}118	α	$1.8^{+75}_{-1.3}$ ms	0.4 ms	11.65 ± 0.06
^{293}116	α	61^{+57}_{-20} ms	80 ms	10.54 ± 0.06
^{292}116	α	18^{+16}_{-6} ms	40 ms	10.66 ± 0.07
^{291}116	α	$6.3^{+11.6}_{-2.5}$ ms	20 ms	10.74 ± 0.07
^{290}116	α	15^{+26}_{-6} ms	10 ms	10.85 ± 0.08
^{289}114	α	$2.6^{+1.2}_{-0.7}$ s	2 s	9.82 ± 0.05
^{288}114	α	$0.80^{+0.27}_{-0.16}$ s	0.9 s	9.94 ± 0.06
^{287}114	α	$0.51^{+0.18}_{-0.10}$ s	0.5 s	10.02 ± 0.06
^{286}114	$\alpha : 40,\ f : 60$	$0.16^{+0.07}_{-0.03}$ s	0.2 s	10.20 ± 0.06
^{285}112	α	29^{+13}_{-7} s	50 s	9.15 ± 0.05
^{284}112	f	97^{+31}_{-19} ms		≤ 9.67
^{283}112	$\alpha, f \leq 10$	$4.0^{+1.3}_{-0.7}$ s	3 s	9.54 ± 0.06
^{282}112	f	$0.50^{+0.33}_{-0.14}$ ms		≤ 10.67
^{281}Ds	f	$11.1^{+5.0}_{-2.7}$ s		≤ 8.87
^{279}Ds	$\alpha : 10,\ f : 90$	$0.18^{+0.05}_{-0.03}$ s	0.2 s	9.70 ± 0.06
^{275}Hs	α	$0.15^{+0.27}_{-0.06}$ s	0.8 s	9.30 ± 0.07
^{271}Sg	$\alpha : 50,\ f : 50$	$2.4^{+4.3}_{-1.0}$ min	0.8 min	8.53 ± 0.08
^{267}Rf	f	$2.3^{+98}_{-1.7}$ h		≤ 8.09

Data on the decay properties of ^{286,287}114, ^{282,283}112 and their descendant nuclei are summarized in table 2. Included also are the data for heavier isotopes with $Z =$ 110–118 that we produced earlier in the reactions ^{244}Pu, ^{245,248}Cm, ^{249}Cf + ^{48}Ca [1,3,8]. The α and SF decay branching ratios, experimental and calculated half-lives and α-particle energies are given. Expected values of $T_\alpha^{\rm calc}$ were calculated from the measured Q_α from the Viola-Seaborg formula [9]. Parameters were fitted to the T_α *vs.* Q_α values of 65 previously known even-even nuclei with $Z > 82$ and $N > 126$. The limiting values of E_α for the SF nuclei were estimated in the same way. The measured half-lives closely reproduce the calculated ones for the even-even as well as even-odd isotopes of elements 112–118 that consequently have rather low hindrance factors, if any, for α decay. For the isotopes of lighter elements, the difference between measured and calculated T_α values increases resulting in hindrance factors of about 10 for ^{279}Ds. One can suppose that in this region of nuclei, a noticeable transition from spherical to deformed shapes occurs at $Z = 100$, in agreement with results observed for odd-Z nuclei [10]. Thus, the decay properties of the isotopes of element 114 are generally determined by the spherical shells $Z = 114$ and $N = 184$. According to the macroscopic-microscopic (MM) model calculations [11],

the nucleus $^{287}114$ is almost spherical ($\beta_2 = 0.088$). In a succession of sequential α decays, the descendant nuclei move away from the closed $N = 184$ shell and approach the deformed shell at $N = 162$. The terminating nucleus, ^{267}Rf ($N = 163$), is deformed ($\beta_2 \sim 0.23$) [11].

Experimental α-decay energies of the isotopes with $Z = 100$–118, together with the decay energies of the same nuclides calculated in the MM nuclear model [11,12], are compared in fig. 4. The experimentally measured values of Q_α practically coincide with theoretical predictions for the deformed nuclei in the vicinity of neutron shells $N = 152$ and $N = 162$ and becomes somewhat less than the calculated values by ≤ 0.5 MeV for the more neutron-rich nuclides with $N \geq 169$. In the decay chain $^{291}116 \rightarrow \ldots \rightarrow {}^{267}$Rf, we observed a similar variation in α-decay energies as we reported for decay chains starting with $^{287}115$ or $^{288}115$ [10]. The slope of Q_α *vs.* neutron number remains practically the same for elements 112–116 but increases significantly for the nuclides with $Z = 111$ and 110. Such an effect might be caused by the transition from spherical nuclear shapes to deformed shapes during successive α decays, in agreement with MM calculations [11]. One should note that the predictions of other models within the Skyrme-Hartree-Fock-Bogoliubov [13] and the relativistic mean field [14] methods also compare well with the experimental results.

If the theoretical predictions of the existence of closed nuclear shells in the domain of superheavy elements are correct, particularly the stronger influence of the closed neutron shell at $N = 184$, they should be characterized not only by high stability to various decay modes (longer half-lives) but also by a relatively high probability of production.

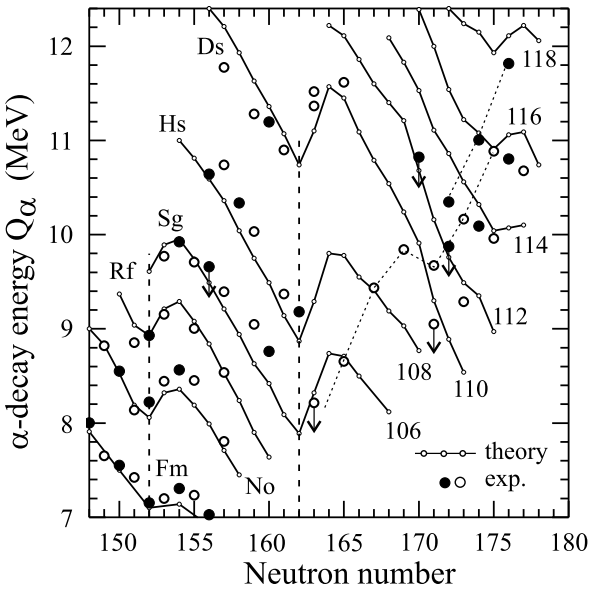

Fig. 4. α-decay energy *vs.* neutron number for isotopes of even-Z elements with $Z \geq 100$ (solid circles: even-even isotopes; open circles: even-odd isotopes) [15,16,17]. Data at $N \geq 163$ that are connected by dashed lines are from [1,3,8] and the present work. Solid lines show the theoretical Q_α values [11,12].

The production of evaporation residues is determined by the probability of the formation of a compound nucleus and the survival probability in the de-excitation to the ground state by emission of neutrons and γ-rays. From numerous experiments it is known that in the synthesis of heavy nuclei with $Z \geq 102$, both in hot and cold fusion reactions, the cross-section σ_{ER} decreases rapidly with increasing Z_{CN}. Extrapolating the dependence $\sigma_{ER}(Z_{CN})$ to $Z > 110$, we would arrive at extremely low cross-sections for the production of isotopes of element 114 ($\sigma_{ER} \sim 1$–10 fb). However, the experimental values of $\sigma_{ER}(Z_{CN} = 114)$ observed in the reactions ^{242,244}Pu + ^{48}Ca appeared to be about 3 orders of magnitude higher.

In cold fusion reactions, the decrease of σ_{ER} with increasing Z_{CN} is associated with the dynamic hindrances of the fusion of massive nuclei [7]. Here, extrapolation to superheavy nuclei appears to be justified, as the hindrances should increase with increasing mass and nuclear charge of the projectile. In asymmetric hot fusion reactions, there are practically no fusion limitations. Here, the decrease of σ_{ER} for higher Z_{CN} is determined by the decreasing survivability of the compound nuclei. The last value strongly depends on the difference between fission barrier B_f and neutron separation energy B_n in the compound nucleus. Since the value of B_f is completely determined by the amplitude of the shell correction ($B_f^{LD} \approx 0$ for the nuclei with $Z \geq 102$), it strongly depends on the neutron number of the compound nucleus. The high fission barriers and correspondingly high cross-sections σ_{ER} observed in the synthesis of elements with $Z = 102$–106 are associated with the significant shell effects at $N = 152$ and at $N = 162$ (fig. 5). For heavier nuclei with $N > 162$, B_f values decrease until the next spherical shell at $N = 184$ starts influencing the fission barrier while B_n values steadily decrease in this region of nuclei. Upon approaching this shell, the fission barriers will increase again. That should result in a substantial increase of σ_{ER}.

As we have shown in fig. 5, the increase of the height of fission barriers due to the influence of the shell closure at $N = 184$ is expected only for the neutron-rich nuclei with $N > 170$. For these nuclei, an increase of the neutron number in the compound nucleus results in an increase of the production cross-section observed in the experiments. We consider this to be the major advantage of using the complete-fusion reactions involving the neutron-rich transuranic target nuclei and the ^{48}Ca projectile for the synthesis of superheavy elements.

Indeed, the experimental data show that for the nuclei with $Z = 112$ and 114 and $N_{CN} = 174$–178 the cross-section of the $4n$-evaporation channel (an "open" channel, well above the fusion barrier) systematically increases with increasing neutron number and reaches the maximum value of about 5 pb in the reaction ^{244}Pu + ^{48}Ca. The low cross-section for the formation of the isotope $^{278}112$ in the reaction ^{233}U + ^{48}Ca with $N_{CN} = 169$ has the same explanation. Additionally, in the reaction ^{248}Cm + ^{48}Ca ($Z_{CN} = 116$ and $N_{CN} = 180$), one could expect a higher σ_{4n} cross-section. At present, this experiment is in progress.

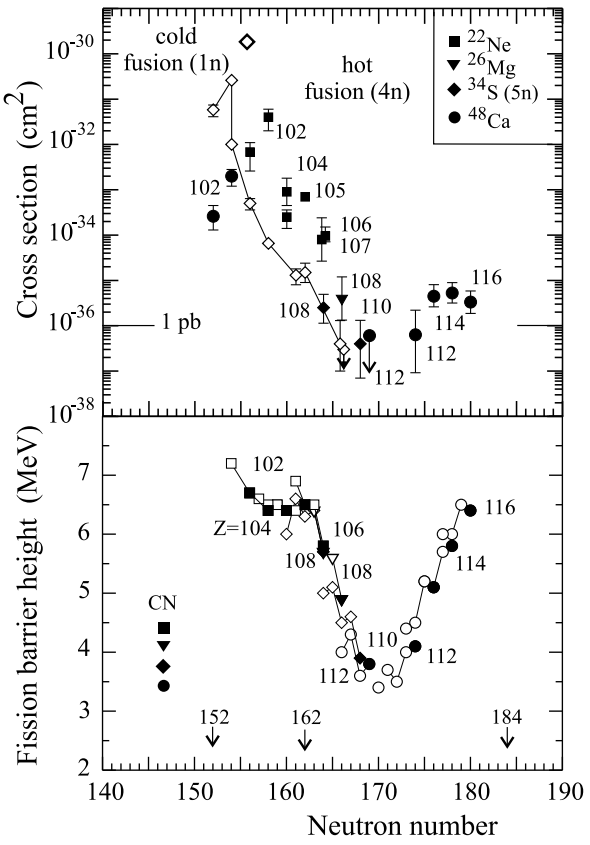

Fig. 5. Comparison of cold fusion and hot fusion cross-sections for the production of $Z \geq 102$ nuclides using a variety of heavy-ion beams (top panel). We show the fission barrier heights of corresponding compound nuclei and neutron-evaporation products as a function of neutron number on the bottom panel [18]. The number of neutrons in compound nuclei formed in different reactions are shown by solid symbols.

The cross-section of the reaction ^{248}Cm(^{48}Ca, $4n$)^{292}116 at $E^* = 38.9$ MeV (about 3 MeV below the expected maximum cross-section for the $4n$-channel) has already reached the value $3.3^{+2.5}_{-1.4}$ pb. In this reaction, six decay chains of the new isotope ^{292}116 were observed. The decay properties of ^{292}116 are also included in table 2.

This work has been performed with the support of the Russian Ministry of Atomic Energy and grant of RFBR No. 04-02-17186. The ^{233}U and ^{242}Pu target material were provided by RFNC-VNIIEF, Sarov, Russia. The ^{248}Cm target material was provided by the U.S. DOE through ORNL. Much of the support for the LLNL authors was provided through the U.S. DOE under Contract No. W-7405-Eng-48. These studies were performed in the framework of the Russian Federation/U.S. Joint Coordinating Committee for Research on Fundamental Properties of Matter.

References

1. Yu.Ts. Oganessian *et al.*, Phys. Rev. C **62**, 041604(R) (2000); Phys. At. Nucl. **63**, 1679 (2000); Phys. Rev. C **63**, 011301(R) (2001); Phys. At. Nucl. **64**, 1349 (2001); Eur. Phys. J. A **15**, 201 (2002).
2. M.G. Itkis *et al.*, *Proceedings of International Workshop on Fusion Dynamics at the Extremes, Dubna, Russia, 2000*, edited by Yu.Ts. Oganessian, V.I. Zagrebaev (World Scientific, Singapore, 2001) p. 93; J. Nucl. Radiochem. Sci. (Jan.) **3**, 57 (2002).
3. Yu.Ts. Oganessian *et al.*, Phys. Rev. C **69**, 054607 (2004).
4. Yu.Ts. Oganessian *et al.*, *Proceedings of the Fourth International Conference on Dynamical Aspects of Nuclear Fission, Častá-Papiernička, Slovak Republic, 1998* (World Scientific, Singapore, 2000) p. 334; K. Subotic *et al.*, Nucl. Instrum. Methods Phys. Res. A **481**, 71 (2002).
5. W.D. Myers, W.J. Swiatecki, Nucl. Phys. A **601**, 141 (1996).
6. R. Bass, *Proceedings of the Symposium on Deep Inelastic and Fusion Reactions with Heavy Ions, West Berlin, 1979*, edited by W. von Oertzen, Lect. Notes Phys., Vol. **117** (Springer-Verlag, Berlin, 1980) p. 281.
7. V.I. Zagrebaev, M.G. Itkis, Yu.Ts. Oganessian, Phys. At. Nucl. **66**, 1033 (2003); V.I. Zagrebaev, *Proceedings of the Tours Symposium on Nuclear Physics V, Tours, France, 2003* (AIP, New York, 2004) p. 31.
8. Yu.Ts. Oganessian *et al.*, JINR Communication D7-2002-287 (2002); Lawrence Livermore National Laboratory Report, UCRL-ID-151619 (2003).
9. V.E. Viola jr., G.T. Seaborg, J. Inorg. Nucl. Chem. **28**, 741 (1966).
10. Yu.Ts. Oganessian *et al.*, Phys. Rev. C **69**, 021601(R) (2004).
11. I. Muntian *et al.*, Acta Phys. Pol. B **34**, 2073 (2003); Phys. At. Nucl. **66**, 1015 (2003).
12. R. Smolańczuk, A. Sobiczewski, *Proceedings of XV Nuclear Physics Divisional Conference "Low Energy Nuclear Dynamics", St. Petersburg, Russia, 1995* (World Scientific, Singapore) p. 313; R. Smolańczuk, Phys. Rev. C **56**, 812 (1997).
13. S. Ćwiok, W. Nazarewicz, P.H. Heenen, Phys. Rev. Lett. **83**, 1108 (1999); J.F. Berger, D. Hirata, M. Girod, Acta Phys. Pol. B **34**, 1909 (2003); S. Typel, B.A. Brown, Phys. Rev. C **67**, 034313 (2003).
14. M. Bender, Phys. Rev. C **61**, 031302 (2000); P.-G. Reinhard *et al.*, *Proceedings of the Tours Symposium on Nuclear Physics IV, Tours, France, 2000* (AIP, New York, 2001) p. 377; Z. Ren, Phys. Rev. C **65**, 051304(R) (2002).
15. R.B. Firestone, V.S. Shirley (Editors), *Table of Isotopes*, 8th ed. (Wiley, New York, 1996).
16. Ch.E. Düllmann *et al.*, Nature **418**, 859 (2002).
17. S. Hofmann, G. Münzenberg, Rev. Mod. Phys. **72**, 733 (2000); S. Hofmann *et al.*, Eur. Phys. J. A **14**, 147 (2002); Z. Phys. A **354**, 229 (1996).
18. R. Smolańczuk, J. Skalski, A. Sobiczewski, Phys. Rev. C **52**, 1871 (1995); I. Muntian, Z. Patyk, A. Sobiczewski, Acta Phys. Pol. B **34**, 2141 (2003).